

A number of abstracts submitted for the 1996 Annual Meeting of the Society of Nuclear Medicine were reviewed only by the Berson-Yalow committee and not by the committee for the specific scientific category. Therefore, those abstracts reviewed only by the Berson-Yalow committee were assigned to a special poster session at this year's annual meeting in Denver, CO. The "walking poster" session with those participants who agreed to present their work was one of the better discussions during the week and showed the widespread influence of Drs. Berson and Yalow, extending from their original *in vitro* studies to the current *in vivo* applications. We do hope that the special poster session and the publication of the abstracts give each applicant's work the recognition it deserves. The following pages should be included as part of the 1996 *May Abstract Proceedings Book* and have been numbered accordingly.

SNM Scientific Program Committee

No. 1800

LONG-TERM OUTCOMES OF 60 BREAST CANCER PATIENTS EXAMINED WITH [16 alpha IODINE-123] IODO-ESTRADIOL 17 beta AND SPECT IMAGING. D.E. Preston, J.A. Spicer, R.J. Baranczuk, M.L. Schiefelbein, K.G. Baxter, M.L. Redick, N.L. Martin. Kansas University Medical Center, Kansas City, KS

Our purpose was to determine the sensitivity, specificity, positive and negative predictive values of I-123 estradiol (I123E2) as a radiotracer to detect breast cancer.

Sixty-six SPECT scans in 60 women with breast cancer or a high risk of breast cancer using high specific activity ($>37 \times 10^7$ MBq(10,000 Ci)/mMol) I123E2. Since 1986 patients were referred from Oncology clinic and a High Risk Breast Cancer Program. Presence, location, and type of breast disease was established by autopsy, biopsy, breast aspiration, estrogen receptor assay, and clinical follow-up. Ages ranged from 20 to 81 and averaged 47. Follow-up exceeded 250 patient years. Average follow-up was 4.7 years.

Patients received stable iodine for 3 days to block the thyroid. Following informed consent, 1.48 MBq(40 uCi)/kg of high specific activity I-123 estradiol was injected intravenously. 2 hours later SPECT imaging (64x64, 64 stops, 40 seconds/stop, LEAP collimation, Orbiter) of the thorax and breasts was begun. Image reconstruction was by filtered back projection (Butterworth .35 order 5). Ratios of breast to lung and axilla to lung were calculated. 56 studies were technically satisfactory. 12 patients were lost to follow-up. 44 patients had sufficient follow-up for analysis.

Sensitivity of .88, specificity of .86, positive predictive value of .78, negative predictive value of .92 were obtained. Estrogen receptor positive and cancers called estrogen receptor negative were identified by I123E2. One cancer was identified 2 years prior to clinical detection. 2 cancers were identified months prior to clinical detection. Focal breast and axillary collections of I-123 twice the lung activity was diagnostic of breast cancer. High positive and negative predictive values and early detection of breast cancer are possible.

No. 1801

PHARMACOLOGICAL AND SPECT EVALUATION OF [I-123]-TPCNE, A SELECTIVE RADIOLIGAND FOR THE SIGMA-1 RECEPTOR. R.N. Waterhouse*, H.F. VanBrocklin, S.M. Hanrahan, J.L. Eberling, S. Jordan and W.J. Jagust. *ANSTO, Lucas Heights, Australia and Lawrence Berkeley National Laboratory, Berkeley, CA.

In recent years sigma (σ) receptors have received attention due to their implicated role in various neurological processes. Several groups have reported the synthesis of σ receptor imaging agents. We report here the further evaluation of [I-123]-1-(iodopropen-2-yl)-4-(4-cyanophenoxy-methyl)piperidine ([I-123]TPCNE), a moderately lipophilic ($\log P_{7.5} = 3.4$) σ -1 selective receptor ligand ($K_i \sigma-1 = 0.67$ nM; $K_i \sigma-2 = 39$ nM).

TPCNE is selective for the σ system as it does not bind dopamine, serotonin, PCP, muscarinic, or NMDA receptors as seen in *in vitro* receptor assays ($K_i > 10,000$ nM). Maximum brain uptake (~2% ID) in male Australian Albino Wistar rats occurred 5 minutes post injection with no significant loss of radioactivity over 4 hours. Brain uptake was blocked 90-95% by σ binding ligands (haloperidol, DUP 734 and unlabeled TPCNE). Pretreatment with either 5HT₂, 5HT_{1C}, D₂, M₁, M₂ or M₃ ligands did not alter brain uptake.

Two dynamic SPECT studies in rhesus macaques were performed using a multidetector scanner. Following a slow bolus injection of ~370 MBq (10 mCi) of [I-123]TPCNE, repeated sequences of 4 coronal slices (180 s of data acquisition) were obtained approx. every 15 min. Imaging was carried out over the first 4 h on day 1 and from 21-24 h on day 2.

Images showed rapid (0-15 min) brain uptake with concentration throughout the cerebral cortex and the cerebellum. Minimal uptake was seen in the basal ganglia and intermediate uptake was seen in the thalamus. By 3 h the activity in the basal ganglia had diminished. At 21 h the activity profile in the brain showed little change from the 3 h images. The distribution of [I-123]TPCNE corroborates our studies in the rat and reported *in vitro* autoradiographic studies in primates (Mash and Zabetian, *Synapse* 12:195-205, 1992). Labeled blood metabolites measured during these studies were minimal. These studies indicate that [I-123]TPCNE is a promising SPECT radioligand for the examination of σ -1 receptor densities. (Supported in part by DE-AC03-76SF00098)

No. 1802

EFFECT OF HYPERTHERMIA ON THE *IN VITRO* UPTAKE OF Ga-67, Tl-201 AND H-3-FDG IN HUMAN CANCER CELLS. A.C. Clavo and R.L. Wahl. University of Michigan Medical Center, Ann Arbor, MI.

Gallium citrate (Ga-67), fluorodeoxyglucose (FDG-18), and thallium chloride (Tl-201) are radioactive tracers commonly used for monitoring cancer therapy, while hyperthermia is increasingly being used as an adjuvant to either radiation or chemotherapy for cancer treatment. Consequently, we exposed human cancer cells to mild (43°C) or severe (56°C) hyperthermia prior to measuring the cellular uptake of the above mentioned tracers to determine hyperthermic effects on tracer utilization. Measurement of tracer incorporation into six human cancer cell lines (melanoma, ovarian carcinoma, breast carcinoma, small cell carcinoma of the lung, lymphoma and squamous cell carcinoma) was conducted in parallel for the above mentioned tracers. Cells were first incubated at varying temperatures (37, 43 and 56°C) for 45 minutes; then uptake was measured after a 30-minute exposure to each tracer at 37°C. When compared to basal conditions (normal 37°C), cellular uptake of FDG and Tl-201 was unchanged in cell lines exposed to 43°C and apparently viable (mean increase of $16.6\% \pm 14.4$; $p = ns$ for FDG and $13.4\% \pm 13.5$; $p = ns$ for thallium) but sharply decreased at the highest temperature of 56°C (mean decrease of $93.2\% \pm 0.5$; $p < 0.0001$ for FDG and $91.8\% \pm 2.7$; $p < 0.0001$ for thallium). By contrast, Ga-67 uptake was greatest in each cell line tested when cells were incubated at 56°C and cellular viability was lowest (mean increase of $639\% \pm 150$; $p = 0.0003$). We conclude that in the malignant human cell lines we tested, the cellular uptake of FDG parallels that of Tl-201 (high in viable cells, low in non-viable cells), while Ga-67 uptake is paradoxically opposite (low in viable cells, high in non-viable cells). Thus, loss of cell viability as a result of hyperthermia seems best monitored by FDG or Tl-201, while Ga-67 has the highest level of uptake in non-viable cancer cells.

No. 1803

Ga-67 and In-111 LABELED FOLATE-CHELATE CONJUGATES FOR TARGETING TUMOR-ASSOCIATED FOLATE BINDING PROTEIN (FBP). C.J. Mathias, S. Wang,* D.J. Waters,† P.S. Low,* and M.A. Green. Departments of *Chemistry, †Veterinary Clinical Sciences, and Medicinal Chemistry, Purdue University, West Lafayette, IN.

The tumor cell membrane-associated folate receptor is a potential molecular target for selective radiopharmaceutical delivery to ovarian, endometrial, and other tumors that overexpress FBP. To better characterize the previously reported Ga-67-labeled deferoxamine-folate conjugate (Df-Folate) a dose escalation study was carried out using athymic mice bearing subcutaneous folate-receptor-positive human KB cell tumors. The Ga-67 labeled Df-Folate was administered via the femoral vein at doses of 133, 27, 2.8, 0.29, and 0.030 mg/kg body mass and animals sacrificed at 4 hours post-injection for quantification of tracer biodistribution. Tumor uptake of Ga-67-Df-Folate decreases at doses above 0.29 mg/kg (presumably due to competitive

receptor binding by the unlabeled excess Df-Folate), dropping from 8.5 ± 0.4 %ID/g tumor ($n = 4$) at the 0.29 mg/kg dose to only 0.96 ± 0.17 %ID/g tumor ($n = 4$) at the 133 mg/kg dose. Tumor/blood, tumor/liver, and tumor/kidney ratios were highest at the 2.8 mg/kg dose with values of 290 ± 60 , 24 ± 7 , and 0.8 ± 0.2 , respectively. At all doses >20% of the tracer was cleared into the intestines. As a strategy to possibly reduce hepatobiliary clearance of the folate-chelate conjugate, a DTPA-Folate conjugate was prepared using ethylenediamine as an amide-linked bridge between a DTPA carboxylate and the γ -carboxylate of folic acid. The In-111 labeled DTPA-Folate conjugate was obtained in high yield by ligand exchange from In-111-citrate. The radiochemical purity of the In-111-DTPA-Folate was determined by thin layer chromatography on C18 eluted with methanol and found to exceed 98% (In-111-DTPA-Folate $R_f = 0.8$; In-111-citrate $R_f = 0.0$). In cultured KB cells the In-111-DTPA-Folate was found to exhibit folate-receptor-dependent cell uptake. A biodistribution study with normal rats showed the In-111-DTPA-Folate to be rapidly excreted into the urine with only 3.7 ± 1.4 % of the dose in the intestines at 4 hours, a value ten-fold lower than observed with Ga-67-Df-Folate in the rat. The In-111 labeled DTPA-Folate conjugate may offer advantages over Ga-67-Df-Folate as a radiopharmaceutical for tumor imaging due to a more favorable pattern of clearance from non-target tissues.

No. 1804

Synthesis and In Vivo Evaluation of In-111 Labeled Paclitaxel: Implications for Tumor Imaging. C. Li, T. Inoue, D-F Yu, D.J. Yang, W. Tansey, M. Diaz, L. Milas, L. R. Hunter, S.S. Kim, D. Podoloff, S. Wallace. Division of Diagnostic Imaging and Division of Radiotherapy, The University of Texas M. D. Anderson Cancer Center., Houston, TX

Paclitaxel, an antineoplastic agent which stabilizes microtubules and arrests cells in G2/M phase, has show activity against ovarian and breast tumors. In order to evaluate the potential value of radiolabeled paclitaxel as an imaging tool in tumors, we synthesized In-111-DTPA-paclitaxel and investigated its biodistribution and γ -scintigraphic imaging properties. Mice bearing both paclitaxel-sensitive tumors (MCA-4, OCA-1) and paclitaxel-resistance tumors (SCC and FSA) were used. In-111-DTPA was used as control. DTPA-paclitaxel was labeled with In-111 with radiochemical yield of 84% and radiochemical purity of 90%. Each mouse received (i.v.) 5 μ Ci of radiotracers for biodistribution studies or 100 μ Ci for γ -scintigraphic studies. In all tumor models, In-111-DTPA was characterized by rapid clearance from the plasma with negligible retention in the tumor, the liver, and other body parts. In contrast, In-111-DTPA-paclitaxel exhibited a pharmacological profiles resembling that of paclitaxel. Furthermore, a significant uptake of In-111-DTPA-paclitaxel was observed in all four murine tumors. In MCA-4 mammary tumors, the tumor/muscle ratios were 2.64, 3.16, and 6.94 at 30 min, 2 hr and 24 hr, although absolute uptake in tumor decreased from 1.95% (injected dose/g) at 30 min to 0.21% at 24 hr after injection. Gamma-scintigraphy clearly showed the retention of radiolabeled paclitaxel in the tumor at 24 hr after injection. In other tumor models, the biodistribution and imaging properties of In-labeled paclitaxel was similar to our findings in MCA-4 murine tumor.

These studies suggest that In-111-DTPA-paclitaxel may be clinically useful to study the uptake of paclitaxel in solid tumors. In tumors where paclitaxel uptake is observed, further studies are necessary to determine whether the tumors will respond to paclitaxel therapy.

No. 1805

PHARMACOLOGIC INTERVENTION MIBG IMAGING WITH UPTAKE-1 INHIBITOR, IMIPRAMINE

Shigetoshi Wakasugi, Terumi Hashizume, Atushi Noguchi, Keijiro Ibusa, Yoshihisa Hasegawa. The Center for Adult Diseases, Osaka, Japan

Assessment of cardiac neuronal uptake-1 activity is clinically important issue because uptake-1 is the main means for terminating the actions of catecholamines in the human heart. Pharmacologic intervention MIBG imaging with pretreatment of uptake-1 inhibitor, imipramine (IMP) may provide a new approach to assess uptake-1 function. I-123-MIBG studies (planar and SPECT imagings) with IMP were performed within 2 months after control studies in 26 normal cases. IMP 25 mg was orally given 2 hr. before i.v. of MIBG. Total injected dose was calculated from dynamic images (1 frame/sec. for 1 min.) and %uptake (counts/pixel/total dose) in the heart, lung and mediastinum were calculated from static planar images at 5 min., 30 min. and 2 hr. after i.v. of MIBG. IMP pretreatment decreased only slightly initial % heart uptake (11.7 ± 10.7 % of control value, $p < 0.0001$) and initial heart to mediastinum uptake ratio (5.3 ± 10.1 % of control, $p < 0.05$), but markedly decreased initial % lung uptake (35.1 ± 15.1 % of control, $p < 0.0001$) and initial lung to mediastinum uptake

ratio (30.0 ± 12.7 % of control, $p < 0.0001$). Initial heart to lung uptake ratio was markedly increased (31.6 ± 15.0 % of control, $p < 0.0001$) and initial % mediastinum uptake was only slightly decreased (6.7 ± 9.0 % of control, $p < 0.005$). However, mean washout rate (SPECT) from the heart was dramatically increased with IMP pretreatment (from 4.7 ± 2.8 %/hr. to 14.2 ± 4.5 %/hr., $p < 0.0001$). Washout rate (planar) in early phase from 5 min. to 30 min. after i.v. of MIBG was more markedly increased from 10.6 ± 6.6 %/hr. to 23.8 ± 8.0 %/hr. ($p < 0.0001$), compared to washout rate in late phase (from 4.8 ± 2.5 %/hr. to 7.7 ± 2.8 %/hr., $p < 0.0002$). These results suggest that: (1) The magnitude of uptake-2 component (extraneuronally localized MIBG) is increased and MIBG washout is accelerated by IMP pretreatment in normal cases with intact uptake-1 function. (2) Alterations of washout rate of MIBG from the heart with IMP pretreatment may reflect uptake-1 activity. (3) Pulmonary uptake of MIBG is more specifically dependent on uptake-1 component compared to cardiac uptake.

No. 1806

CAN F-18 FLUOROMISONIDAZOLE DETECT RADIO-RESISTANT TUMOR IN VIVO?

K. Kubota, M. Tada, S. Yamada, R. Iwata, and K. Sato. Tohoku University, Sendai, Japan

The binding of F-18 fluoromisonidazole (FMISO) to hypoxic cells has been reported mainly by in vitro studies. In order to examine in vivo characteristics of FMISO, the feasibility for the detection of radio-resistant tumor and intra-tumoral distribution of FMISO were studied using rat AH109A tumor model. Time course tissue distribution of FMISO in rats showed the highest uptake by liver followed by kidney. Blood, lung, heart, muscle, and brain are the third group of uptake level. All normal tissues showed slow exponential clearance patterns after initial accumulation with the T1/2 about 2hr. Tumor uptake reached a plateau at 30 min remained constant up to 2 hr, and decreased. The uptake patterns suggest some metabolic interaction between FMISO and tumor but not normal tissues. Solid tumors were produced on both sides of thighs. To induce tumor ischemia, ligation of the right proximal thigh was performed under anesthesia. Tumor on the left thigh served as the control. After ligation, tumor blood flow decreased from 26.0 ± 5.0 to 4.8 ± 1.7 ml/min/100g tissue ($n=8$ each) by hydrogen gas clearance method. Radiotherapeutic response of the ischemic tumor showed early regrowth compared to the control. The growth delay was 63% of the control after 10, and 20 Gy of radiotherapy. Mean uptake of FMISO by ischemic tumors is lower than the control at 60 min. Only 4 of the 11 rats at 120 min, showed higher FMISO uptake by ischemic tumor than the control. Double tracer autoradiography of tumor showed that the area of high FMISO uptake showed low uptake of C-14 methionine (Met), while low FMISO uptake area showed high Met uptake. The detection of radioresistant tumor by FMISO uptake is not reliable. Opposite distribution patterns of FMISO and Met suggested the interesting characteristics of flow dependency of tracers uptake.

No. 1807

HIGH INCIDENCE OF CCK-B/GASTRIN RECEPTORS IN HUMAN MEDULLARY THYROID CANCERS AND SMALL CELL LUNG CANCERS: DIFFERENTIAL DIAGNOSTIC IMPLICATIONS. J.C. Reubi. Division of Cell Biology and Experimental Cancer Research, Institute of Pathology, University of Berne, Switzerland.

Peptide, (i.e. somatostatin) receptor imaging is a powerful diagnostic tool for the in vivo tumor localization. Cholecystokinin (CCK) and gastrin are two other regulatory peptides with trophic functions, acting through CCK-A and/or CCK-B/gastrin receptors. 175 human tumors were therefore evaluated with in vitro receptor autoradiography for their CCK-A and/or CCK-B receptor content. CCK-A receptors were identified with a 125 I-CCK-decapeptide analog (125 I-D Tyr]-Gly[Nie 28,31]CCK 26-33) displaced by nanomolar concentrations of CCK but not by gastrin. CCK-B/gastrin receptors were identified: 1) with 125 I-Lau 15 -gastrin, displaced by nanomolar concentrations of gastrin; 2) with the 125 I-CCK decapeptide analog displaced by nanomolar concentrations of gastrin.

Whereas most of the tested gastrointestinal tumors (25 colon and gastric cancers) did not express significant amounts of CCK-A or CCK-B receptors, a high incidence of CCK-B receptors was found in two types of neuroendocrine tumors: 14/21 small-cell lung cancers (SCLC) and, unexpectedly, 21/23 medullary thyroid cancers (MTC). CCK-A were not expressed in these tumors except for 2 MTC. The high expression of CCK-B receptors is selective for MTC and SCLC compared to the non-medullary thyroid cancers (0/11 CCK-receptor positive) and the NSCLC (1/11 CCK-B-receptor positive). Moreover, other neuroendocrine tumors (pituitary

adenomas, pheochromocytomas, paragangliomas, neuroblastomas, parathyroid adenomas) rarely expressed the CCK-A or the CCK-B receptors, except for GEP tumors bearing the CCK-A receptor in 9/30 cases and CCK-B receptor in 6/30 cases.

CCK-B receptors in MTC and SCLC may have the following implications: 1) they may be of interest for nuclear medicine as targets for the in vivo imaging of these tumors with labeled CCK analogs; the high incidence of CCK-B receptors in MTC and SCLC compared to non-MTC, NSCLC, and other neuroendocrine tumors may have differential diagnostic value. 2) they may be of biological significance and play a role in the growth regulation of these tumors. Moreover, CCK-B receptor antagonists may be of therapeutic interest in these tumors.

No. 1808

SENSITIVITY IMPROVEMENT IN In-111 PENTETREOTIDE ONCOLOGY SPECT STUDIES USING A FAST MULTIPLICATIVE ALGORITHM.

S. Walrand, L. van Elmbt, S. Pauwels. Department of Nuclear Medicine, University of Louvain Medical School, Brussels, Belgium.

In low count rate In-111 pentetreotide studies, reconstruction with the Filtered Backprojection (FBP) shows artificial null activity between organs of high activity, e.g. kidney, spleen, liver. Such artifact hampers the detection of abdominal tumours and may result in a lower sensitivity compared to planar views. This drawback can be circumvented by the EM-ML algorithm that provides accurate determination of activity in low count regions, even in the vicinity of more active organs. However, EM-ML requires long computation time, especially to visualize small low count lesions. Recently, we developed and validated on Tc-99m phantoms, an accelerated modified version of the EM-ML algorithm, namely the False Likelihood (FL), which has a high convergence speed over the full image. In the present study, the FL was evaluated both in phantom and clinical SPECT studies with In-111 pentetreotide.

Application of the FL algorithm on an anatomical phantom of the abdomen with activity similar to usual clinical conditions, allowed to see small sources of 1.5 cm diameter located near a large source with a specific activity 15 times higher. In contrast, FBP reconstruction allowed only to see small sources 4 times less active than the large one.

The FL algorithm was subsequently evaluated on 13 patients with a known tumour located near the kidneys or the spleen. For all patients the lesion contrast obtained with FL was much better compared to EML or planar views. Improvement of lesion delineation was noticed in 5 studies. In 2 cases FL reconstruction confirmed the lesions detected on the planar views, while FBP was negative.

In conclusion, on the basis of phantom and clinical studies, the FL algorithm seems well suitable to In-111 pentetreotide studies.

No. 1809

EXTRACTION AND RETENTION OF THALLIUM AND RUBIDIUM IN ISOLATED RABBIT HEART. R. C. Marshall, S. E. Taylor, P. Powers-Risius, B. W. Reutter, A. Kuruc, R. H. Huesman and T. F. Budinger. Lawrence Berkeley National Laboratory, Berkeley, CA.

The purpose of this study was to provide a quantitative comparison of myocardial extraction and retention of the potassium analogues thallium and rubidium and compare potential inaccuracies in their use as myocardial flow tracers.

We studied 21 isolated, isovolumic retrograde red blood cell/albumin perfused rabbit hearts at plasma flow rates ranging from 0.5 to 2.7 mL min⁻¹ gm⁻¹. Rapid venous sampling was initiated simultaneously with the introduction of a mixed bolus of I-125 albumin, Tl-201, and Rb-83 through a side-port just above the aortic cannula. Deconvolution of the Tl and Rb venous output curves by the albumin venous output curve was used to separate the effects of circulatory dispersion, as reflected in the albumin curve, from the effects of myocardial extraction and retention of Tl and Rb. The resulting impulse responses for Tl and Rb quantified the uptake and retention of these tracers by the myocardium. The deconvolution process was stabilized by constraining the estimated impulse responses to be nonnegative and nonincreasing.

The mean initial extraction of Rb was slightly higher than that of Tl, 72% vs. 65%. However, there was much more rapid washout of Rb than Tl, 32% vs. 6% of the total tracer amount in the 5-to-30-second time interval. The tails of the impulse responses were closely approximated by a single decaying exponential with mean time constant of 20 and 21 minutes for Rb and Tl, respectively. The mean area under exponential fits to these tails was 2 times greater for Tl than Rb, 62% vs. 29% of the total injected amount. These areas were both negatively correlated with perfusion rates with a slope of -11% per mL min⁻¹ gm⁻¹.

We interpreted the area under the exponential fits as representing tracer that

is temporally retained in the heart, probably in the myocyte. The results are consistent with Rb having slighter greater access to the interstitial space, but significantly less efficient uptake in myocytes than Tl. The negative correlation of myocyte uptake with perfusion rates is consistent with non-flow-limited (barrier limited) uptake of the potassium analogues Tl and Rb by myocytes.

Work supported by U.S. Department of Health and Human Services Grant No. HL25840 and DOE Contract No. DE-AC03-76SF00098.

No. 1811

SEX DIFFERENCES IN HUMAN MU OPIOID RECEPTOR BINDING DETECTED BY PET AND [C-11] CARFENTANIL

J.K. Zubietta*, Y.R. Smith*, H.T. Ravert, R.F. Dannals, J.J. Frost. Johns Hopkins University, Baltimore, Maryland. *Current Affiliation: University of Michigan, Ann Arbor.

Sex and age-related differences in human normal and pathological brain functions have been described, but the neurochemical mechanisms underlying these differences are currently unknown. We measured μ -opioid receptor binding in the brains of healthy human subjects with PET and [C-11]carfentanil (CFN). Thirty subjects, 12 men and 18 women, aged 19-79 years, were scanned with a GE4096 PET camera after i.v. administration of 740 \pm 70 MBq [C-11]CFN. Reproductive age women were studied in the follicular phase of the menstrual cycle. Subject positioning in the PET scanner, and region of interest placement in the PET images, were standardized by coaligning the PET imaging plane with CT images of the subject. ANCOVA demonstrated higher μ opioid binding in women compared to men in neocortical regions, caudate, thalamus, amygdalae and cerebellum. Women-men differences ranged from 8 to 69% during the reproductive years ($p < 0.05$). In postmenopausal women the differences became less prominent, with μ binding approaching levels similar to those of age-matched men in most brain regions. Indeed, ANCOVA detected significant age-by-gender interactions in the amygdalae and thalamus ($p < 0.05$), where postmenopausal women showed binding levels below those of age-matched men. In addition, μ opioid binding increased with advancing age in neocortical regions and putamen ($p < 0.001$). These increases ranged from 36 to 89% from the 3rd decade of life to the 7th decade or older. These data imply that both sex and age are important variables to consider in the interpretation of brain function studies in which the opioid system may play a role. Additionally, that hormone-mediated alterations in the opioid system during the menopause may be involved in the cognitive and affective changes described during this phase of human aging.

No. 1812

MU OPIOID RECEPTOR BINDING IN WOMEN: RELATIONSHIP WITH NEUROPSYCHOLOGICAL TESTING SCORES.

J.K. Zubietta*, Y.R. Smith*, P.M. Maki, M.G. Del Carmen, D. Schretlen, J. Brandt, H.T. Ravert, R.F. Dannals, J.J. Frost. Johns Hopkins University, Baltimore, Maryland. *Current Affiliation: University of Michigan, Ann Arbor

Sex differences in neuropsychological test performance have been described, but their neurochemical bases are not well understood. Prior studies by our group have shown sex differences in μ opioid receptor binding, with women showing higher binding than men. Animal studies have also shown that μ binding changes during the normal estrous cycle. In this study we tested the hypothesis that μ binding is modulated during the normal menstrual cycle, and that regional μ receptor densities may be associated with specific cognitive measures. We measured μ opioid receptor binding in 10 young (19-32 years old) right-handed healthy women. Subjects were scanned during both the follicular and luteal phases, with a GE4096 PET camera after i.v. administration of 740 \pm 70 MBq [C-11]carfentanil, a selective μ ligand. Neuropsychological testing of verbal, spatial, mood and motor functions were obtained prior to both scanning periods. Subject positioning in the PET scanner, and region of interest placement in the PET images, were standardized by coaligning the PET imaging plane with CT images of the subject. Paired t-tests did not show significant differences in μ binding between follicular and luteal phases ($p > 0.05$). Data pooled from both scanning periods revealed that verbal and non-verbal learning and delayed recall scores were positively correlated with μ binding in the amygdalae, while motor skills were correlated with thalamic binding (Pearson correlations, $p < 0.05$). Conversely, mood ratings were negatively correlated with ventral caudate and frontal cortex binding ($p < 0.05$). These data do not support the hypothesis that μ

opioid receptor binding varies during the menstrual cycle. On the other hand, our data do suggest that the endogenous opioid system is involved in the modulation of cognition, mood and motor function in healthy women.

No. 1813

Characterisation of Three [I-123]-labeled Sigma Receptor Ligands as Potential Tumor Imaging Agents for SPECT. Rikki N. Waterhouse, Beverley Izard and Kerynne Belbin. Australian Nuclear Science and Technology Organisation, Lucas Heights, Australia

It has been reported that sigma (σ) receptors are found in a wide variety of human tumors. These findings have stimulated research into the development of radiolabeled σ receptor ligands for use in tumour tomographic imaging. We have synthesised and characterised three selective sigma receptor ligands [I-123]-1-(*trans*-iodopropen-2-yl)-4-(4-cyanophenoxyethyl)piperidine, ([I-123]TPCN; $K_i \sigma_1 = 0.67$ nM, $K_i \sigma_2 = 39$ nM), [I-123]-1-(4-cyanobenzyl)-4-(*trans*-iodopropen-2-ylmethoxy)piperidine ([I-123]CNBN; $K_i \sigma_1 = 0.38$ nM, $K_i \sigma_2 = 21$ nM) and [I-123]-1-(2-hydroxyethyl)-4-(4-cyanophenoxyethyl)piperidine ([I-123]HEPIE; $K_i \sigma_1 = 2.3$ nM, $K_i \sigma_2 = 139$ nM). All three ligands were prepared via oxidative iododestannylation methods and specific activities >77,000 MBq/ μ mol were obtained. Radiochemical yields were routinely 60-80% EOS and radiochemical purities were >99%. All three ligands were evaluated in nude mice with B16 melanoma tumors. The tumor uptake of radioactivity was moderate to high, with maximum uptake occurring at 2 hours post-injection (3.93 ± 1.03 ID/g for [I-123]CNBN, 7.82 ± 2.25 ID/g for [I-123]TPCNE and 12.25 ± 2.06 for [I-123]HEPIE ($n = 5$)). There was no significant loss of radioactivity from the tumors for up to 24 hours. In the B16 melanoma model, the most promising results were obtained using [I-123]HEPIE for which tumour/tissue ratios (ID/g) were positive by 8 hours PI for most organs and increased thereafter. In subsequent studies, [I-123]HEPIE was evaluated in nude mice with A375 human malignant melanoma and U87 MG human glioblastoma tumors. These tumors were initiated in the flank just below the skin and ranged from 4-10 mm in diameter. The results obtained indicate that [I-123]HEPIE has potential as a SPECT imaging agent for the detection of malignant melanoma and glioblastoma.

Tumour/Tissue ratios (%ID/g) at 24 hrs post-injection for [I-123]HEPIE

Tumour	Blood	Muscle	Brain	Lung	GIT
B16 malignant melanoma	54.7	22.8	5.2	5.3	5.7
A375 malignant melanoma	18.9	7.2	1.9	1.4	2.0
U87 MG glioblastoma	17.2	7.4	1.5	1.4	1.7

No. 1814

Synthesis and Characterisation of [F-18]-1-(3-Fluoropropyl)-4-(4-cyanophenoxyethyl)piperidine ([F-18]FPCN): A Potential Sigma-1 Receptor Ligand for PET. Rikki N. Waterhouse, T. Lee Collier, Joanne O'Brien. Australian Nuclear Science and Technology Organisation, Lucas Heights, NSW, Australia

In recent years sigma (σ) receptors have received attention due to their implicated role in certain neurological processes. To date, the determination of the biological functions of σ receptors has been hampered in part by the lack of σ receptor subtype selective ligands. To prepare a potential PET radiotracer for the measurement of σ -1 receptor densities, FPCN was synthesised and examined in *in vitro* receptor binding assays. FPCN was determined to be selective for the σ -1 receptor subtype ($K_i \sigma_1 = 4.3$ nM, $K_i \sigma_2 = 144$ nM) and did not bind ($K_i > 10,000$ nM) to dopamine, serotonin, PCP, muscarinic or NMDA receptors. Furthermore, FPCN has adequate lipophilicity ($\log P_{7.5} = 2.8$) for high brain uptake and low non-specific binding.

[F-18]FPCN was prepared by reacting the corresponding mesylate precursor with [F-18]fluoride at 85°C in acetonitrile in the presence of kryptofix K222 and potassium carbonate. The reaction was complete in 15 minutes and the radioligand was obtained in 70-80% yield (EOS) after HPLC purification. The radiochemical purity was determined to be >99% and the specific activity was >74,000 MBq/ μ mol (EOS).

The whole body distribution of [F-18]FPCN was examined in male Australian Albino Wistar rats. The maximum brain uptake of radioactivity (2.38 ± 0.33 %ID) occurred at five minutes post-injection and no significant loss of radioactivity occurred over the course of the study (4 hours). Examination of the regional brain distribution of the [F-18]FPCN indicated that the density of radioactivity was highest in the posterior cortex > frontal cortex > cerebellum and other brain regions. In all brain regions, most of the uptake was inhibited by pre-administration (1mg/kg) of compounds with affinity for σ receptors, including haloperidol, Dup 734 and unlabeled FPCN. In contrast, the uptake of radioactivity was not altered by pre-treatment with ritanerin (5HT₂, 5HT_{1C}), S(-)-eticlopride (D₂) or atropine (M₁, M₂, M₃). The results of these *in vivo* and *in vitro* studies indicate that [F-18]FPCN is a potential PET radioligand for the examination of σ -1 receptor densities.

No. 1815

SYNTHESIS AND BIOLOGICAL ACTIVITY OF RADIOLABELED DTPA-COBALAMIN ANALOGUES. D.A. Collins and H.P.C. Hogenkamp. Mayo Clinic, Rochester, MN, and University of Minnesota, Minneapolis, MN.

Malignant cells upregulate the number of transcobalamin II receptors during DNA replication. Currently *in vivo* transcobalamin II receptor imaging of tumors is not possible because of the low specific activity (16.5-37 kBq/ μ g) and long half life (270.9 days) of Co-57-cyanocobalamin. **Methods:** Methyl-, adenosyl-, and cyanocobalamin-b-(4-aminobutyl)-amide-DTPA analogues were synthesized. Chelation of Tc-99m, In-111, and Gd-153, as well as the specific activity of the analogues was assessed via thin layer chromatography and autoradiography. *In vitro* biological activity of the analogues was assessed by Unsaturated Vitamin B₁₂ Binding Capacity (UBBC) and Intrinsic Factor Blocking Antibody (IFBA) assays. DTPA and cyanocobalamin underwent UBBC and IFBA assays for comparison. *In vivo* biodistribution of In-111-DTPA-cobalamin was compared with In-111-DTPA in tumor and non-tumor bearing female Balb-c mice. **Results:** At a concentration of 370 Mbq/ μ g, there was 99.9% efficiency in chelation of Tc-99m by the DTPA-cobalamin analogues ($n=7$). The attachment of DTPA to cyano-, methyl- and adenosylcobalamin does not greatly affect their interaction with the transcobalamin proteins. However, it does affect their interaction with Intrinsic Factor. Compared with In-111-DTPA, the In-111-DTPA-cobalamin analogues had 5-12 times greater uptake within the harvested organs and tissue; with 10-20 times the amount of uptake in the transplanted murine sarcomas. **Conclusion:** The radiolabeled DTPA-cobalamin analogues are biologically active, and may be effective for *in vivo* transcobalamin II receptor imaging.

No. 1816

[I23]CARAZOLOL AS A RADIOLIGAND FOR THE IMAGING OF CARDIAC β -ADRENOCEPTORS USING SPECT. E.A. Dubois, G.A. Somsen, J.C. van den Bos, A.G.M. Janssen, M. Pfaffendorf, E.A. van Royen, P.A. van Zwieten. Academic Medical Centre, Amsterdam, The Netherlands.

In patients with heart failure sympathetic activity is increased and cardiac β -adrenoceptors (β -AR) are downregulated. Reduction of this neurohormonal activation is related to improved prognosis. To evaluate therapeutic strategies, it would be of clinical importance to measure cardiac β -AR density non-invasively.

The present study was designed to develop a radioligand to image β -AR using SPECT. (S)-4-(3-(1,1-Dimethyl-3-iodo-2E-propenylamino)-2-hydroxypropoxy)carbazole (CYBL8E), which is an iodinated derivative of carazolol, was evaluated both *in vitro* and *in vivo*. Using homogenates of cardiac left ventricular tissue (LV) of male New Zealand White rabbits and [125I]iodocycano-pindolol, the K_i value of this compound for the receptor was determined at 0.31 ± 0.03 nmol.l⁻¹, versus 0.76 ± 0.10 for CGP12177 (mean \pm S.E.M., $n=3-5$). Subsequently, the biodistribution and specific binding *in vivo* was studied. Anaesthetized rabbits received 50 μ Ci CYBL8E (specific activity > 5000 Ci/mmol), intravenously. Animals were killed at several time points after injection. Radioactivity levels measured in lung (L) and LV are listed in the table. Data are expressed as % injected dose x kg body weight/g tissue (mean \pm S.E.M.).

	LV (n=3)	Lung (n=3)	LV (n=3)	L (n=3)
5 min	0.52 ± 0.09	5.75 ± 0.38	4 h	0.14 ± 0.03
30 min	0.26 ± 0.02	1.74 ± 0.14	6 h	0.09 ± 0.004
1 h	0.20 ± 0.004	1.43 ± 0.21	24 h	0.02 ± 0.001
2 h	0.20 ± 0.03	1.29 ± 0.21		0.18 ± 0.01

In additional experiments animals were pretreated with 0.1 μ mol of the antagonists IC118,551, atenolol, CGP12177, or (-)-propranolol, 10 minutes prior to the administration of the radioligand. Atenolol, CGP12177 and (-)-propranolol significantly reduced LV uptake by 36%, 64%, and 59%, respectively. IC118,551 slightly increased LV uptake. IC118,551, atenolol, CGP12177, and (-)-propranolol significantly reduced L uptake by 43%, 64%, 66%, and 55%, respectively. These data demonstrate that CYBL8E may be a suitable SPECT radioligand.

No. 1817

STAGING OF SMALL CELL LUNG CANCER (SCLC) WITH IN-111 PENTETREOTIDE SCINTIGRAPHY. COMPARISON WITH WHOLE-BODY PET-FDG. M. Lonneux, F. Jamar, R. Bausart, M. Sibomana, N. Leners, Y. Humblet, Ph. Collard and S.

Pauwels. PET Laboratory and Dept. of Medicine, Univ. of Louvain Medical School, Brussels, Belgium.

We prospectively evaluated the efficacy of somatostatin receptor imaging (SRI) and whole-body PET-F-18-FDG in the staging of small cell lung cancer (SCLC). Ten consecutive patients with newly diagnosed SCLC were studied. Conventional staging included physical examination, liver enzymes, chest X-ray, chest and brain CT, bone scan and liver CT or US. Bone marrow biopsy was obtained after SRI (n=10) and PET-FDG (n=9) studies.

The final stage was defined after confirmation by appropriate means of additional SRI or FDG findings, and was limited in 2 and extended in 8 pts. As shown in Table, SRI correctly staged 8/8 extended disease and falsely upgraded one limited disease. PET correctly staged 9/9 patients.

Final stage	n	conventional staging	SRI	PET-FDG
extended	8	7/8	9/8	7/7
limited	2	3/2	1/2	2/2

Sites				
contralat	6	6/6	8/6*	5/5
liver	6	6/6	2/6	6/6
brain	2	1/2	1/2	1/2
adrenals	2	1/2	1/2	2/2
marrow	6	6/6	6/6	5/5

* 1 heterolat. node, 1 pleural plaque

PET-FDG and SRI both proved accurate in the staging of SCLC, especially for the assessment of bone marrow involvement. These preliminary data also suggest that PET-FDG might be superior to SRI due to higher sensitivity for detection of liver or adrenal lesions, and the absence of false positive sites.

No. 1818

PRELIMINARY IMAGING STUDY OF HUMAN NEUROBLASTOMA WITH INDIUM-111-LABELLED ANTISENSE OLIGONUCLEOTIDES IN NUDE MICE. N. Mataraba¹, K. Endo¹, H. Sawai², K. Shinozuka², H. Ozaki², K. Higuchi², Y. Shirakami³. Department of Nuclear Medicine, Faculty of Medicine¹, Department of Chemistry, Faculty of Engineering², Gunma University, Gunma, Nihon Medi-Physics³, Chiba, Japan

Antisense oligonucleotide is potentially an approach to diagnosis and therapy for malignant disease. Activation of oncogenes by means of amplification leads to an increased amount of the mRNA transcript in the cytoplasm. The aim of the study is to localize malignant tumor expressing a particular mRNA transcript with radiolabeled antisense oligonucleotide. Antisense chimeric phosphodiester oligonucleotide(o) and antisense chimeric monothioester oligonucleotide(s)(15 mer) to the translation start region of N-myc mRNA were prepared using a newly developed C-5 substituted uracil nucleosides. Indium-111-chloride was bound to the antisense oligonucleotide via DTPA-anhydride with labeling efficiency of above 85 % and specific activity of 34MBq/mg. T_{1/2} of antisense(o) or (s) in human normal serum was 4.0 hr or more than 48 hr, respectively. Melting temperatures of antisense (o) and (s) conjugated with DTPA were 64.6°C and 54.2°C, whereas that of antisense (o) without DTPA was 65.6°C. ¹¹¹In-DTPA-antisenses were intravenously administered into each two nude mice with human neuroblastoma expressing N-Myc. Tumor image could be obtained, however, antisense(o) showed 7.2 % ID/g in the transplanted tumor, whereas antisense (s) demonstrated 0.08 % ID/g, paradoxically. Our preliminary data did not show specific accumulation of ¹¹¹In-DTPA-antisense (s) in the transplanted tumor.

No. 1819

GG918 IS A HIGH POTENCY MODULATOR OF MDR1 P-GLYCOPROTEIN-MEDIATED TRANSPORT OF Tc-99m-Q-63 AND Tc-99m-SESTAMIBI. C.L. Crankshaw, G. Luker, V.V. Rao, and D. Flivnick-Worms. Washington University Medical School, St. Louis, MO.

MDR1 P-glycoprotein (Pgp) recognizes Tc-99m-Q-63 [trans[5,5'-(1,2-ethanediyldiimino)bis(2-OEt-2-Me-4-penten-3-one)] bis(dimethyl(3-

OMe-1-propyl)phosphine]Tc(III)] and Tc-99m-SESTAMIBI, lipophilic cationic radiopharmaceuticals, as avid transport substrates at picomolar concentrations. Glaxo-Wellcome GG918 is a new high potency reversal agent of Pgp. To characterize modulation of Pgp-mediated transport of Tc-99m-Q-63 and Tc-99m-SESTAMIBI, GG918 was tested in human epidermal carcinoma KB-3-1 cells and the colchicine-selected MDR KB-8-5. These cells express non-immunodetectable and modestly low levels of MDR1 Pgp, respectively, by Western blot analysis with mAb C494. Net uptake (30 min) of Tc-99m-Q-63 was inversely proportional to Pgp expression levels: 316 ± 36 and 6 ± 0.6 fmol/mg prot/nM₀ (mean ± SEM; n=4 each), respectively, as was Tc-99m-SESTAMIBI: 341 ± 36 and 7.2 ± 0.9. GG918 showed no tracer enhancement in KB-3-1 cells, but induced full reversal of both tracers in KB-8-5 cells with an EC₅₀=50 nM. By comparison, cyclosporin A also had no effect in KB-3-1 cells, but reversed tracer accumulation in KB-8-5 cells with an EC₅₀ value 40-fold higher (2 μM for both tracers). Furthermore, GG918 enhanced Tc-99m-Q-63 and Tc-99m-SESTAMIBI net uptake in Sf9 cells infected with baculoviral constructs containing wild-type recombinant human MDR1 (EC₅₀=50 nM), but not mock-infected or MDR3-infected cells. These data indicate that GG918 is a high potency modulator of MDR1 Pgp-mediated Tc-99m-Q-63 and Tc-99m-SESTAMIBI transport at concentrations identical to those reported for GG918-mediated cytotoxic modulation (Cancer Res 53:4595, 1993) and further support use of combination Tc-99m-Q-63/GG918 or Tc-99m-SESTAMIBI/GG918 for analysis of Pgp transport function in vivo ("modulator challenge test") and as surrogate markers of MDR cytotoxic modulation in cancer patients.

No. 1821

ANIMAL STUDIES ON THE REDUCTION OF 2-DEOXY-2[18]FLUORO-D-GLUCOSE (FDG) ACTIVITY IN THE KIDNEYS AND EXCRETION IN THE URINE. S. Kosuda, S. Fisher, R.L. Wahl. University of Michigan, Ann Arbor, MI.

One of the limitations of FDG imaging in patients with genitourinary neoplasms is intense F-18 activity in the kidneys and excretion in the urine. The aim of our study was to evaluate in a rodent model, several methods to potentially reduce and/or dilute the FDG activity in the urine.

In the L-lysine study, five male Sprague-Dawley rats were injected with L-lysine intraperitoneously 4 times, starting from 60 minutes before FDG injection, and then at 30 minute intervals for 90 minutes. The dose of L-lysine was 2,500 ug/g per injection. As a control study, 5 rats were treated as above, using saline. The injected dose of FDG was approximately 7.4 MBq, each. Another study was a furosemide study. 12 rats were allocated into 3 groups, with intraperitoneal injection of furosemide (7 mg/Kg, once) plus saline (one 30th of the body weight per injection, 3 times) (group 3), saline only with the same protocol (group 2) before the FDG injection, and control (group 1). The renal uptake of FDG with pre-treatment of L-lysine was higher than that with saline. Lasix administration also increased renal F-18 concentration from 0.0442±0.0030 (control, group1) to 0.0767±0.0049 %Kg.inj.dose/g (lasix plus saline, group3), but the administration of lasix plus saline (group 3) decreased urinary concentration and the administration of saline only (group2) further decreased it beyond that with lasix plus saline. Urinary F-18 concentrations (with metabolic cage collections) were (%Kg injected dose/g): 5.28±2.05 in group 1, 0.522±0.290 in group 2, 1.49±0.76 in group 3.

In conclusion, it was not possible to lower the renal FDG accumulation by L-lysine or lasix in our animal study. However, an administration of saline without lasix before the FDG injection did not lower renal activity but appeared to significantly reduce urinary activity, and should have a potential for improving the pelvic image quality of the FDG PET in patients with genitourinary neoplasms.

No. 1822

BIODISTRIBUTION OF MUSCARINIC SUBTYPE SELECTIVE AGONISTS OF THE THIADIAZOYL TETRAHYDROPYRIDINE CLASS. D.O. Kiesewetter, E. Jagoda, R.E. Carson, P. Herscovitch, W.C. Eckelman. PET Department, National Institutes of Health, Bethesda, MD.

We have synthesized, radiolabeled with F-18, and evaluated 3-(3-(2-fluoroethylthio)-1,2,5-thiadiazol-4-yl)-1,2,5,6-tetrahydro-1-methylpyridine [FE-TZTP], and 3-(3-(3-fluoropropylthio)-1,2,5-

thiadiazol-4-yl)-1,2,5,6-tetrahydro-1-methylpyridine [FP-TZTP] for muscarinic subtype selectivity. Preliminary *in vitro* data suggested that FP-TZTP had a 7 fold selectivity for M2 over M1, while FE-TZTP had a 12 fold selectivity for M2 over M1 (J. Med. Chem. 1995, 38, 5). More detailed studies show a two component binding curve. However in rats, [F-18] FE-TZTP displays lower uptake *in vivo* and is blocked only weakly by unlabeled P-TZTP. *In vitro* FE-TZTP shows only weak affinity to sigma receptors and it is not blocked *in vivo* upon co-injection with haloperidol. In contrast, [F-18]FP-TZTP shows significant blocking of uptake by unlabeled P-TZTP. No blocking of uptake of [F-18]FP-TZTP is observed with the M1 antagonist (R,R)-IQNB. Uptake of [F-18]FP-TZTP is quite rapid peaking at 15 min; the clearance proceeds quickly with the cerebellar activity approaching that in the blood by two hours. Clearance is slower in the medulla and pons, tissues containing a higher proportion of M2 subtype. Analysis of metabolites in the rat brain reveal that the parent compound represents >86% of the activity in the brain at 15 min.

In vivo studies using [F-18]FP-TZTP in rhesus monkey revealed two lipophilic metabolites which represent 30% of the blood activity at 20 min. However, based on the above rat metabolism results, we believe that metabolites are not present in monkey brain to a significant extent up to 45 min. Brain uptake is rapid and the clearance is sustained over 2 h. Administration of P-TZTP or FP-TZTP (83 nmol/kg) at 60 min results in a rapid displacement of brain activity in all tissues. The studies in monkeys are consistent with our results in rat and support our hypothesis that [F-18]FP-TZTP is a M2 selective ligand.

No. 1823

SYNTHESIS AND BIODISTRIBUTION OF THE MUSCARINIC RECEPTOR ANTAGONISTS (R,R)- AND (R,S)-FLUOROMETHYL QNB. D. O. Kiesewetter, E. Jagoda, R.E. Carson, C.J. Endres, P. Herscovitch, W.C. Eckelman. PET Department, NIH, Bethesda, MD.

We have developed a multistep radiochemical synthesis of quinuclidinyl-4-[F-18]fluoromethylbenzilate (FMeQNB). The two diastereomers (R,R) and (R,S) display opposite *in vitro* selectivity for muscarinic subtypes. The (R,R) displays an 8 fold selectivity for M1 while (R,S) displays a 7 fold selectivity for M2 (J. Med. Chem. 1995, 38, 1711). This compound displays a slow decomposition in saline. In the rat, uptake of (R,S)-FMeQNB is nearly uniform in all brain regions following the concentration of M2 subtype. The uptake is blocked by about 50% in all brain regions upon coinjection with 50 nmol of cold ligand. An injection of (R,S)-FMeQNB followed at 60 min by injection of cold ligand and subsequent kill at 120 min shows a 30 to 50% displacement of radioactivity in all brain regions. The most dramatic displacement and blocking of (R,S)-FMeQNB is observed in the heart. Displacement in the heart using (R,S)-FMeQNB or (R)-QNB is nearly 80%. (R,R)-FMeQNB shows a very different pattern of uptake in brain regions that correlates with the M1 subtype population. Displacement with (R)-QNB shows a more varying amount displaced. In the heart, which is primarily M2, the uptake is only 0.2% ID/g and shows only a 50% reduction following the blocking dose. In rhesus monkey (n=4), (R,S)-FMeQNB shows prolonged brain uptake and retention. In the blood, the parent compound degrades rapidly; within 30 min the parent is less than 5% of the blood activity. Kinetic analysis of brain ROIs showed moderate extraction ($K_1 \sim 0.1$ ml/min/ml) with nearly irreversible behavior in cortical and sub-cortical regions ($k_4 < 0.005$ /min) but not in cerebellum ($k_4 > 0.1$ /min). Displacement with (R)-QNB is greater from those brain regions that contain a higher proportion of the M2 subtype. Compared to control data, QNB displacement (n=2) reduced radioactivity concentration by 50%, 35-38%, 26%, and 14% in thalamus, cortical regions, basal ganglia, and cerebellum, respectively. (R,S)-[F-18]FMeQNB displays M2 selectivity based on our studies in both rats and monkeys.

No. 1825

A METHOD FOR THE RADIOHALOGENATION OF INTERNALIZING ANTIBODIES. C. J. Reist, P. K. Garg, K. L. Alston, D. D. Bigner, and M. R. Zalutsky. Departments of Radiology and Pathology, Duke University Medical Center, Durham, NC.

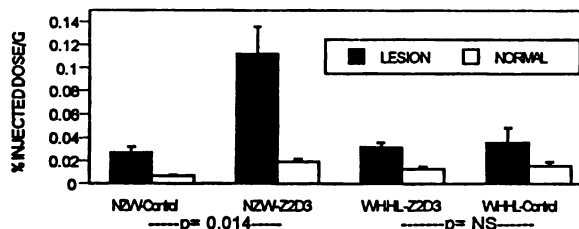
Maximizing radiation dose to tumor with internalizing monoclonal antibodies (MAbs) requires an approach where the labeled catabolite created is retained in the cell following intracellular processing. Since lysosomes are known to retain positively charged compounds, N-

succinimidyl 5-iodopyridinecarboxylate (SIPC) might be ideal for this purpose because of the positive charge on the pyridine ring. In addition, the known catabolites 5-iodonicotinic acid (INA) and its lysine conjugate are excreted very rapidly, minimizing normal tissue activity levels. L8A4, a MAb directed against the mutant epidermal growth factor receptor variant III (EGFRvIII) which rapidly internalizes after binding, was labeled with ¹²⁵I using SIPC and ¹³¹I using either Iodogen or N-succinimidyl 3-iodobenzoate (SIB). *In vitro* studies demonstrated up to 65% increased intracellular retention of activity in HC2 20D2 cells, a line transfected to express EGFRvIII, with SIPC labeling. The possible role of charge influencing cellular retention is supported by the results of distribution coefficient experiments which indicate that about 10 times more INA compared with 3-iodobenzoic acid molecules are charged at lysosomal pH. Reverse-phase HPLC catabolite analyses confirmed the presence of INA and INA-lysine in lysates from cells incubated with SIPC labeled L8A4. Paired-label tissue distribution studies demonstrated that the tumor uptake of L8A4 was enhanced significantly by SIPC labeling ($32.7 \pm 2.0\%$ ID/g, SIPC; $24.4 \pm 2.2\%$ ID/g, Iodogen, at 24 hr). These results suggest that SIPC is a promising method for increasing the tumor retention of this, and possibly, other internalizing MAbs.

No. 1826

PREFERENTIAL UPTAKE OF INDIUM-111-LABELED Z2D3 IN RAPIDLY PROLIFERATING SMOOTH MUSCLE CELLS ENVISIONS CLINICAL UTILITY OF Z2D3 IN PREDICTING RESTENOSIS. J. Narula, A. Petrov, R. Virmani, F. Kolodgie, B.A. Khaw. Northeastern University and Massachusetts General Hospital, Boston, MA; and Armed Forces Institute of Pathology, Washington, D.C.

Proliferation of smooth muscle cells (SMC) and medial extracellular remodeling determines the incidence of restenosis after angioplastic interventions. Since Z2D3 antibody specifically identifies proliferating SMC, we used indium-111-Z2D3 in two experimental models of atherosclerosis for noninvasive imaging and to compare Z2D3 uptake with SMC proliferation rate. The study included 6 Watanabe heritable hyperlipidemic (WHHL) rabbits and 8 NZW rabbits with experimental atherosclerotic lesions (induced by abdominal aorta deendothelialization and 6% peanut oil + 2% cholesterol diet for 8-12 weeks). Indium-111 chimeric Z2D3 or control F(ab)₂ (25-28.5 mBq) were administered i.v. and imaging performed at 0.5, 24 and 48 H. Atherosclerotic lesions were visualized in 3 of the 4 NZW and in none of the WHHL by Z2D3. No lesions were seen in either group with control antibody. Antibody uptake in atherosclerotic lesions and normal aorta was as follows:



This preferential uptake Z2D3 uptake in the angioplastic compared to spontaneous model of atherosclerosis envisions potential clinical utility of Z2D3 for noninvasive assessment of the rate of SMC proliferation.

No. 1827

Comparative Evaluation of Tc-99m MIBI and Tl-201 in Primary Lung Cancer and Predicting Chemotherapeutic Effect by Tc-99m MIBI in Small Cell Carcinoma.

Y. Nishiyama, Y. Yamamoto, K. Fukunaga, Y. Kawasaki, K. Satoh, H. Takashima, and M. Tanabe. Kagawa Medical School, Kagawa, Japan.

Tc-99m MIBI and Tl-201 scintigraphy were performed for examination of positive delineation of primary lesion in 42 patients with histological proved primary lung cancer, and Tc-99m MIBI scintigraphy was done prior to chemotherapy to evaluate correlation between accumulation of Tc-99m MIBI and chemotherapeutic effect in 9 patients with small cell carcinoma. Dual SPECT images of Tl-201 and Tc-99m MIBI

were taken 15 minutes (early image) and 2 hours (delayed image) after intravenous injection of the radiopharmaceuticals. Regions of interest were placed over the tumor area (T) and contra lateral normal lung area (N) and T/N ratio and retention index were calculated. The positive rate was 98% in both the early and delayed images for Tl-201 and 95% in the early and 88% in the delayed image for Tc-99m-MIBI. Both early and delayed T/N ratios for Tl-201 were higher than those for Tc-99m MIBI. The retention index of Tl-201 was higher than that of Tc-99m MIBI. There was a tendency of increase in retention of Tl-201 from small cell carcinoma to squamous cell carcinoma and to adenocarcinoma with an opposite tendency for Tc-99m MIBI. The correlation between accumulation of Tc-99m MIBI and chemotherapeutic effect in small cell carcinomas showed that the T/N ratio in patients with CR and PR was higher than that in those with NC and PD. The retention index in patients with CR and PR was higher than in patients with NC and PD. This preliminary study shows that Tc-99m-MIBI SPECT can be useful for localizing primary lung cancer and for evaluating chemotherapeutic effect in small cell carcinoma.

No. 1828

Tc-SESTAMIBI IS TRANSPORTED BY P-GLYCOPROTEIN AND THE MULTIDRUG RESISTANCE ASSOCIATED PROTEIN. N.H. Hendriks^{1,2}, E.G.E.de Vries¹, W.T.A.van der Graaf¹, C.Meijer², D.A.Piers², W.Vaalburg¹, E.J.F.Franssen^{1,2}. ¹PET Center, ²Departments of Medical Oncology & ³Nuclear Medicine, Groningen University Hospital, The Netherlands.

Resistance of tumors for chemotherapeutic drugs is a major cause of failure of antitumor treatment. One cause of multidrug resistance (MDR) is the presence of the transmembrane drug efflux pump P-glycoprotein (Pgp). Several drugs (e.g. verapamil) can act as modulators for Pgp. Another pump, the multidrug resistance associated protein (MRP) is also involved in cytosolic efflux and is glutathione-mediated. [Tc-99m]-Sestamibi (Tc-MIBI) is a transport substrate for Pgp and may be used for functional imaging of Pgp *in vivo*. Thus far, its pharmacology in MRP-mediated MDR is unknown. Since this may interfere with Pgp imaging, we separately investigated the pharmacology of Tc-MIBI in P-gp and MRP-mediated forms of MDR *in vitro*.

Pgp-pharmacology. The steady state intracellular concentration (SSIC) of Tc-MIBI in a Pgp positive and MRP negative human ovarian carcinoma cell line (2780AD) was 1% of that in its Pgp and MRP-negative control (A2780). The efflux of Tc-MIBI was larger in 2780AD than in A2780. In 2780AD the SSIC of Tc-MIBI was 35 fold enhanced by co-incubation with 50 µM verapamil (in contrast to A2780). These data confirm Pgp-mediated Tc-MIBI pharmacokinetics.

MRP-pharmacology. Human, Pgp negative, lung carcinoma cell lines (GLC4) and MRP overexpressing sublines with different drug resistance factors (GLC4/ADR 2-150x) were used. Increased MRP expression coincided with a decreased SSIC and an enhanced efflux of Tc-MIBI. Depletion of glutathione enhanced the SSIC of Tc-MIBI in GLC4/ADR150x to a level comparable to that in un depleted GLC4. This effect was not observed in GLC4. This indicates glutathione-mediated MRP transport of Tc-MIBI in MDR cells. The IC10 and IC25 of Tc-MIBI in GLC4 were 50 µM and 80 µM respectively. In GLC4/ADR150x the IC10 and IC25 were 100 µM and > 300 µM, respectively. This suggests increased survival due to MRP-mediated efflux of Tc-MIBI. Overall, the data indicate that Tc-MIBI is a transport substrate for Pgp and a(n) direct substrate for MRP. Apart from Pgp imaging, Tc-MIBI may also be used for imaging MRP-mediated drug resistance *in vivo*. Grant: Dutch Cancer Society GUKC 94-783.

No. 1829

LYMPHOSCINTIGRAPHY AND INTRAOPERATIVE GAMMA PROBE DETECTION OF A SENTINEL NODE IN EARLY STAGE MELANOMA.

PC Barneveld, V Bongers, PW de Graaf*, PP van Rijk. Departments of Nuclear Medicine and *Surgery, Utrecht University Hospital, The Netherlands.

Introduction: The value of elective lymph node dissection in early stage melanoma patients (pts) is still controversial. Therefore, we prospectively studied the patterns of tumor-draining lymph nodes (sentinel node, SN) by preoperative lymphoscintigraphy (LS) and intraoperative gamma probe detection.

Methods: LS was performed in 24 pts (12 female, 12 male), with a mean age of 52 years (23-81 yrs), having a malignant melanoma (Breslow thickness 0.45 - 8 mm) on the back (n=8), head (n=4), upper limb (n=4) or lower limb (n=8). An amount of 20-80 MBq Tc-99m-nanocolloid, divided in four equal portions, was injected

intradermally around the scar of the excisional biopsy. The lymph channels (LC) and SNs were visualized during dynamic imaging in the first 20 minutes and by static imaging after 1-2 hours.

Results: In 24 pts we found a total of 37 LCs and 40 SNs. In 4 pts 3 LCs were found, in 7 pts 2 LCs, and 1 LC was found in 11 pts. In 2 pts no LC, but one SN could be detected. All SNs were easily detected during surgery and also *ex vivo* using the gammprobe (TEC PROBE 2000, Stratec, Germany). 37 SNs were explored, because 3 nodes were in an inaccessible site and therefore not operated upon. In 5 cases the direction of lymphatic drainage and the location of the SN was unexpected. Malignancy was found in 7 out of 11 SNs in another 5 pts. **Conclusion:** LS and gammprobe detection allows selective lymphadenectomy in melanoma patients. Moreover, early phase dynamic acquisition is of great value in detecting unexpected LCs and SNs. In this study a radical nodal bed dissection could be prevented in 19 patients with a tumor negative SN. In those pts (n=5) with a malignant SN nodal bed dissection and additional treatment was performed in a later phase.

Key Words: sentinel node, malignant melanoma

Corresponding author: PC Barneveld, Utrecht University Hospital, PO Box 85500, 3508 GA Utrecht, phone +31 30 2507773, fax +31 30 2507785.

No. 1830

[carbonyl-C-11]WAY-100635 — A RADIOLIGAND FOR THE EXQUISITE DELINEATION OF 5-HT_{1A} RECEPTORS IN HUMAN BRAIN WITH PET. Y.W. Pike, J.A. McCarron, A.A. Lammertsma, S. Osman, S.P. Hume, P.A. Sargent, P.M. Grasby, A. Fletcher¹, I.A. Cliffe¹ and C.J. Bench. Cyclotron Unit, MRC CSC, RPMS, Hammersmith Hospital, London, U.K. and ¹Wyeth Research (U.K.) Ltd, Taplow, Berkshire, U.K.

WAY-100635 [N-(2-(4-(2-methoxyphenyl)-1-piperazinyl)ethyl)-N-(2-pyridyl)-cyclohexanecarboxamide] is the first potent and selective antagonist for 5-HT_{1A} receptors. We labelled WAY-100635 in its carbonyl position with carbon-11 (*t*_{1/2} = 20.4 min) for evaluation as a radioligand for the study of 5-HT_{1A} receptors in human brain with PET.

[carbonyl-C-11]WAY-100635 (~7.3 mCi; specific radioactivity, ~2 Ci/µmol) was injected intravenously into each of 5 male healthy volunteers who were then scanned parallel to the orbito-meatal line with PET. The acquired data, summed from 20 to 90 min after radioligand injection, provided exquisite delineation of 5-HT_{1A} receptors in brain, with high uptake in receptor-rich regions including medial temporal lobe, insula, cingulate cortex and the raphe nuclei. The cerebellum, which is virtually devoid of 5-HT_{1A} receptors, had very low uptake of radioactivity such that the ratio of radioactivity in receptor-rich medial temporal cortex to that in cerebellum reached the remarkably high value of 25 by 60 min after injection. This value is ~8 times greater than that previously obtained by using WAY-100635 labelled with carbon-11 in the methoxy position.

Plasma metabolite analysis after radioligand injection into humans shows that [carbonyl-C-11]WAY-100635 forms only very polar radioactive metabolites, which are probably cyclohexane derivatives that are pharmacologically benign and unable to cross the blood-brain barrier, whereas [methoxy-C-11]WAY-100635 is metabolised to the radioactive des-cyclohexanecarbonyl derivative. [methoxy-C-11]WAY-100634, which has high affinity for 5-HT_{1A} receptors and a higher extraction fraction than [C-11]WAY-100635.

It was possible to apply a tracer-kinetic model to the data obtained with [carbonyl-C-11]WAY-100635 and to extract values for binding potential which are as high as 7.8 in receptor-rich regions.

[carbonyl-C-11]WAY-100635 is concluded to be superior to [methoxy-C-11]WAY-100635 as a radioligand for the investigation of 5-HT_{1A} receptors in human brain with PET and for application in neuropsychiatric and pharmacological research.

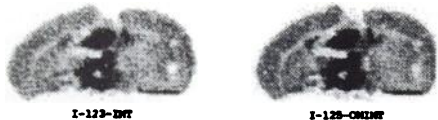
No. 1831

I-123-α-METHYLTYROSINE (IMT) AND I-125-O-METHYL-α-METHYLTYROSINE (OMIMT) AUTORADIOGRAPHY IN A RAT GLIOMA MODEL K.-J. Langen¹, K.Csaplár¹, H. Mühlensiepen¹, K. Ziemons¹, M. Holschbach², J.C.W. Kiwit⁴, K. Zilles⁴, H.-W. Müller-Gärtner^{1,3}. Inst. of Med.¹ and Nucl. Chem.², Research Center Jülich, Dept. of Neuroanatomy³ and Neurosurgery⁴, Univ. of Düsseldorf, Germany.

IMT has proven to be a promising SPECT tracer of amino acid uptake in cerebral gliomas. An analogue of the molecule, OMIMT, showed 5 times higher brain uptake in mice than IMT. The aim of this study was to compare tumor/brain accumulation of IMT and OMIMT.

Cell suspensions of the anaplastic rat glioma clone F98 were inoculated

stereotactically into the brain of six adult Fischer-CDF rats. After 8 days of tumor growth animals were anesthetized and I-123-IMT and I-125-OMIMT injected simultaneously into a tail vein. Animals were killed after 15 min, brains removed and frozen in liquid isopentane. Serial 20 μm sections of the tumor bearing brain area were produced and exposed to photo imager plates immediately and after decay of I-123 radioactivity. IMT and OMIMT distribution images were generated by image subtraction. An example is shown in Fig.1. Tumor/brain ratios are given in Table 1.



Rat	1	2	3	4	5	6	mean ± SD
IMT	2,42	3,9	3,43	2,24	2,40	2,23	2,45 ± 0,48
OMIMT	2,11	2,8	3,16	2,13	2,45	2,22	2,48 ± 0,42 (not significant)

Extent of tumor labelling with IMT and OMIMT was identical in all cases. Tumor/brain ratios for OMIMT were only slightly lower than for IMT in this glioma model. Thus, OMIMT, due to its higher brain uptake, may offer significant reduction of cost and radiation exposure compared to IMT.

No. 1832

DOES TI-201 SCINTIGRAPHY PREDICT PROLIFERATIVE ACTIVITY IN THYROID TUMORS ? K. Nakada, C. Katoh, K. Kanegae, E. Tsukamoto, K. Itoh, N. Tamaki. Hokkaido University School of Medicine, Sapporo, Japan.

Ti-201(Tl) scintigraphy has been used for differentiating benign from malignant thyroid nodules. Based on the reports that Tl uptake indicates the biological characters in brain tumor, we postulate that Tl uptake may predict proliferative activity in thyroid tumor. We undertook comparative study to identify the relationship between the Tl uptake and the tissue proliferation related factor in thyroid tumors. Tl scintigraphy was performed in 39 patients with malignant tumor and in 24 with benign tumor. Static anterior image of the thyroid was obtained at 10 min. (early scan) and 120 min. (delayed scan) following intravenous injection of 37 ~ 74 MBq of Tl. The Tl uptake calculated as tumor / background activity was compared with labeling index for proliferating cell nuclear antigen (PCNA), which was quantitatively determined by flow cytometry using biopsy specimen. PCNA is regarded as a parameter of the cells in S phase. The correlation coefficients between Tl uptake and labeling index for PCNA were:

	early scan	delayed scan
Malignant tumor	r = 0.578*	r = 0.815*
Benign tumor	r = 0.641*	r = 0.826*

*. p<0.001

The correlation between Tl uptake and labeling index for PCNA was significant in both benign and malignant tumors. Such correlation was more prominent in the delayed scan. These data suggest that thyroid tumors with high Tl uptake in the delayed scan include more cells in the S phase regardless of histopathological diagnosis. In conclusion, Tl scintigraphy is useful for predicting proliferative activity of thyroid tumors.

No. 1833

COMPARATIVE STUDY OF XENON-133 GAS DYNAMIC SPECT AND HIGH-RESOLUTION CT IN PULMONARY EMPHYSEMA. K. Takahashi, K. Satoh, Y. Nishiyama, and M. Tanabe. Kagawa Medical School, Kagawa, Japan.

The purpose of this study was of assess the usefulness of Xenon-133 dynamic SPECT (Xenon SPECT) by comparing Xenon-133 washout axial images with high-resolution CT (HRCT) in patients with pulmonary emphysema. Thirteen patients were examined ; all ware male and their mean age was 67, with ages ranging from 49 to 77 years. The patients inhaled 370 MBq Xenon-133 and held their breath for 15 seconds. SPECT imaging was performed using a Picker model Priam 2000. Xenon

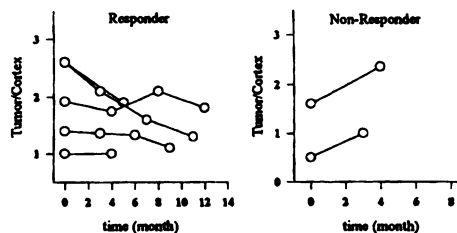
SPECT images were continuously acquired every 60 seconds for 6 minutes. Greater than three minutes' retention of Xe-133 during washout imaging was viewed as abnormal. Axial images were made for the Xe-133 functional map (MTT, T_{1/2}). HRCT images were classified seriousness of illness based on the extent of low attenuation areas. We compared Xe-133 washout functional map with HRCT in the same level axial image. In all patients, more detailed findings were made using Xenon SPECT than using HRCT. In one patient abnormal findings were not made using HRCT, but Xenon-133 retention was observed. Xenon SPECT was more effective in assessing the extent on damage than was HRCT. We conclude that Xenon SPECT is a more effective means of finding ventilation impairment in pummonary emphysema than is HRCT.

No. 1834

I-123-α-METHYLTYROSINE (IMT) SPECT FOR THE EVALUATION OF CHEMOTHERAPY IN CEREBRAL GLIOMAS D. Schmidt³, G. Wunderlich³, K.-J. Langen¹, K. Ziemons¹, J.C.W. Kivit⁴, M. Holschbach², H.-W. Müller-Gärtner^{1,3}. Institutes of Medicine,¹ and Nuclear Chemistry,², Research Center Jülich, Departments of Nuclear Medicine³ and Neurosurgery⁴, University of Düsseldorf, Germany

The evaluation of chemotherapeutic effects in cerebral gliomas with CT and MRI is crucial. The aim of this study was to investigate changes of IMT-uptake in cerebral gliomas during the course of chemotherapy in comparison with clinical course

Seven patients with residual tumor tissue after operation and/or irradiation of cerebral gliomas were studied by IMT SPECT before and during chemotherapy. SPECT scans were done 15 to 60 minutes after intravenous injection of 300 - 500 MBq IMT using a triple headed gamma camera. IMT uptake in the tumours was quantified by tumor/cortex ratios. Patients with a stable clinical course and reduction of tumor volume on MRI/CT scan were classified as responders, patients with tumor progression as non-responders. Changes of the tumor/cortex ratios in the two groups are shown in Fig. 1.



Our preliminary results indicate that changes of IMT uptake in gliomas during chemotherapy are related to clinical response. Thus IMT SPECT may help to guide therapeutic strategy in patients with gliomas.

No. 1835

TUMOR IMAGING WITH THE ESTROGEN RECEPTOR RADIOLIGAND Z-[I-123]MIVE IN PATIENTS WITH METASTATIC BREAST CANCER. L.J.M. Rijks, P.J.M. Bakker, C.H.N. Veenhof, G.J. Boer, K. de Bruin, A.G.M. Janssen, and E.A. van Royen. Department of Nuclear Medicine, Department of Medical Oncology, Academic Medical Center, Amsterdam; Cygne BV, Technical University, Eindhoven, The Netherlands.

In earlier studies Z-118-methoxy-17α-[I-123]iodovinylestradiol-178 (Z-[I-123]MIVE) showed excellent estrogen receptor binding properties both in vitro and in the rat in vivo. In this study the potential of Z-[I-123]MIVE as imaging agent of estrogen receptor-positive breast tumors was investigated. Anterior and posterior whole body scans were made at 1, 2, 4, 6 and 24 h after i.v. injection of 150 MBq Z-[I-123]MIVE (specific activity 200 MBq/nmol) of 7 patients with metastatic breast cancer (age 34 - 71 years). Regions of interest were drawn to calculate the geometric mean counts/pixel in the different lesions. The results were expressed as lesion-to-background uptake ratios. Low lung uptake and rapid hepato-biliary excretion resulted in good imaging conditions for the thorax. Analysis of the abdomen was more difficult due to high uptake in the bowel. Pathologic accumulation of Z-[I-123]MIVE was detected in radiologically and/or scintigraphically confirmed metastases in the lungs, liver, bone, brain and lymph nodes. The lesion-to-background ratios increased over time,

being e.g. at 4 and 24 h after injection in the lungs 2.7 and 3.6, abdominal region 3.7 and 4.3, mediastinal lymph nodes 2.9 and 3.8, other lymph nodes 2.6 and 4.0, liver 3.2 and 4.7, sternum 2.2 and 3.3, and os ilium 3.7 and 6.1. There was also high accumulation of Z-[I-123]MIVE in the thoracic region of 2 patients with known pleuritis carcinomatosa and lymphangitis carcinomatosa. Four patients got a second Z-[I-123]MIVE scan after 2 to 3 weeks of therapy with the anti-estrogen tamoxifen. In all 4 patients no Z-[I-123]MIVE uptake was seen anymore in any of the lesions, due to blockade of the estrogen receptors. This indicates that the tumor uptake of Z-[I-123]MIVE is specific, i.e. estrogen receptor-mediated. In conclusion, Z-[I-123]MIVE accumulates specifically in breast cancer metastases in bone, liver, lung, brain and lymph nodes. Therefore, Z-[I-123]MIVE is a very promising radioligand for the detection and analysis of both primary and metastatic estrogen receptor-positive breast cancer.

No. 1836

IMAGING OF PRIMARY BREAST TUMORS WITH THE ESTROGEN RECEPTOR SPECIFIC RADIOLIGAND Z-[I-123]MIVE. L.J.M. Rijks, G. van Tienhoven, K. de Bruin, G.J. Boer, A.G.M. Janssen, and E.A. van Royen. Depts. Nuclear Medicine and Radiation Oncology, Academic Medical Center, Amsterdam; Cygne BV, Technical University, Eindhoven, The Netherlands.

Z-11 β -methoxy-17 α -[I-123]iodovinylestradiol-17 β (Z-[I-123]MIVE) showed in earlier studies high estrogen receptor binding in vitro and high estrogen target tissue uptake selectivity in the rat in vivo. In healthy human volunteers Z-[I-123]MIVE showed low lung retention, rapid hepato-biliary excretion and diffuse uptake in normal breast tissue. In this study the potential of Z-[I-123]MIVE as diagnostic imaging agent of primary breast cancer was investigated.

Anterior and posterior whole body scans were made at 1, 2, 4 and 6 h after i.v. injection of 150 MBq Z-[I-123]MIVE (specific activity 200 MBq/nmol) of 5 patients with primary breast cancer (estrogen receptor status unknown) and a positive intraclavicular biopsy (age 49 - 78 years). Regions of interest were used to calculate the mean counts/pixel in the primary breast tumor and the tumor-to-background uptake ratio. At 2 and 4 h after injection also static planar acquisition as well as SPECT of the thoracic region were performed.

Low lung uptake and rapid hepato-biliary excretion allowed early imaging of the thorax. Pathologic accumulation of Z-[I-123]MIVE was clearly detected in the primary breast tumors of all 5 patients. The tumor-to-background ratios were the highest at 2 to 4 h p.i., being in the range of 1.3 to 2.8. Although all tumors were visible on the whole body images, image quality improved with static planar acquisition and SPECT. In 2 patients no Z-[I-123]MIVE accumulation could be detected in scintigraphically suspected bone lesions. Further radiological examination (CT) showed indeed no metastatic disease. By contrast, another scintigraphically suspected and afterwards radiologically confirmed bone metastasis showed indeed Z-[I-123]MIVE uptake.

In conclusion, Z-[I-123]MIVE accumulates in primary breast tumors. Moreover, tumor uptake of Z-[I-123]MIVE in metastatic breast cancer patients could be blocked with the anti-estrogen tamoxifen, which indicates that the tumor uptake of Z-[I-123]MIVE is specific, i.e. estrogen receptor-mediated. Therefore, Z-[I-123]MIVE is a very promising radioligand for the analysis and staging of primary breast cancer, and can be helpful to select patients who may benefit from hormonal therapy.

No. 1837

SHIFTING RATE-LIMITING STEP OF GLUCOSE METABOLISM IN TUMOR CELLS A. Waki,

Y. Fujibayashi, Y. Yonekura, N. Sadato, Y. Magata*, T. Tsuchida, Y. Ishii and A. Yokoyama, Fukui Medical School, Fukui, & *Kyoto University, Kyoto, Japan.

To correlate biochemical characters of tumors, such as malignancy, growth rate and cell activity, with FDG-PET images, the relationship between the rate-limiting step of glucose metabolism and FDG accumulation should be clarified. In this study, we examined the accumulation of FDG in LS180, cultured human tumor cells, in comparison with lipophilic FDG analogue, 1,3,4,6-tetra-acetyl-2-[F-18]-2-deoxy-D-glucose (acetyl-FDG) which shows glucose transporter (GLUT) independent penetration into cells but metabolizable to FDG-6-P. FDG showed lower uptake in tumor cells and slower metabolic conversion to FDG-6-P than acetyl-FDG. Extracellular glucose concentration directly influenced accumulation of FDG and production of FDG-6-P but not in case of acetyl-FDG, indicating that GLUT should act as a rate-limiting step of FDG uptake. On the other hand, 2,4-dinitrophenol (DNP), known to induce GLUT protein to plasma membrane, resulted in ca. 2 times higher FDG uptake, with less increment for FDG-6-P production. In this condition, namely under elevated GLUT expression and unchanged expression level of hexokinase protein, hexokinase should be saturated and become a rate-limiting step of glucose metabolism. Decreased acetyl-FDG uptake in GLUT-induced cells also indicated the elevation of intracellular glucose concentration. Gathering these results, shifting the rate-limiting step of glucose metabolism between GLUT and hexokinase was clearly visualized. Combination PET studies with physiological intervention, such as glucose loading, might clarify the biochemical characters in tumors by means of rate-limiting analysis of glucose metabolism.

No. 1838

P-GLYCOPROTEIN MONITORING OF CARBON-11 DAUNORUBICIN AND VERAPAMIL IN P-GLYCOPROTEIN GENE KNOCK-OUT AND WILD TYPE MICE WITH PET. E.J.F. Franssen^{1,2}, N.H. Hendrikse^{1,2}, P.H. Elsinga¹, E. Fluks^{1,2}, A.H. Schinkel¹, W.T.A. van der Graaf¹, A.M.A. van Loenen-Weemaes¹, E.G.E. de Vries¹ and W. Vaalburg¹. ¹PET Center, Departments of ²Nuclear Medicine and ³Medical Oncology, Groningen University Hospital, ⁴Division of Molecular Biology, Dutch Cancer Institute, Amsterdam, the Netherlands.

Resistance against drugs in tumors can be the result of an increased expression of P-glycoprotein (Pgp). This membrane protein actively pumps drugs from tumor cells. This protein is encoded by the *mdr1*-gene. Apart from tumors the gene is expressed in various tissues, such as the brain, testis and liver. For imaging the functionality of Pgp with PET, we are investigating [C-11] daunorubicin (DNR) and verapamil (VER), Pgp transport substrates. To validate whether [C-11] DNR and [C-11] VER are suitable for non-invasive Pgp function measurements in vivo, their pharmacokinetics have been studied in *mdr1* gene-disrupted mice (*mdr1a*^{-/-}) (Schinkel *et al.*, Cell 77:491-502, 1994) and wild-type mice *mdr1a*^{+/+}.

Drug uptake in tissues was measured by ex-vivo counting (60 min post injection) and with PET (0-60 min post injection). Especially in Pgp-rich tissues, such as the brain and testis, differences in drug uptake were observed after administration of [C-11] DNR and VER. For instance, administration of [C-11] DNR (doses: <100 ng/kg and 10 mg/kg) resulted in 50%, respectively 40 % higher brain uptake in *mdr1a*^{-/-} than in *mdr1a*^{+/+} mice. Administration of [C-11] VER (doses <100 ng/kg and 0.1 mg/kg) resulted in 650%, respectively 370% enhanced brain uptake in *mdr1a*^{-/-} as compared to that in *mdr1a*^{+/+} mice. PET studies with [C-11] VER revealed rapid brain uptake of VER in *mdr1a*^{-/-} and no uptake in *mdr1a*^{+/+}. In contrast, PET studies with [O-15] water demonstrated equal brain perfusion in both types of mice. Therefore, the enhanced brain uptake of [C-11] DNR and VER in the *mdr1a*^{-/-} mice is the reflection of reduced drug efflux due to the lack of Pgp in the blood brain barrier. In conclusion, these data demonstrate the potential of C-11 DNR and VER for non-invasive Pgp measurements in vivo with PET. Grant: Dutch Cancer Society GUKC 94-783.

Due to production complications, the following three abstracts were not included in the
JNM Abstract Book Supplement.

No. 1171

TECHNETIUM-99m SESTAMIBI BREAST IMAGING ACCURATELY EXCLUDES BREAST CANCER. P.J. Peller, N.Y. Khedkar, and C.J. Martinez. Lutheran General Hospital, Park Ridge, IL.

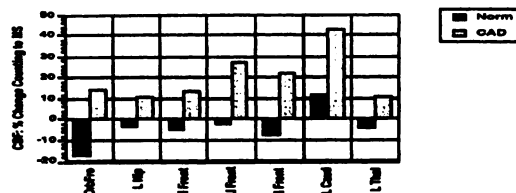
The purpose of this study was to evaluate prospectively the ability of Sestamibi breast imaging to exclude breast cancer in a suspicious breast lesion. Eighty-four consecutive women (age 38.2 ± 1.6 years) referred for a palpable breast mass (N=64) or mammographic abnormality (N=20) underwent prone breast imaging. Immediately after intravenous administration of 740-1110 MBq of Tc-99m Sestamibi, planar views (10 minutes each) of the breast were obtained, right and left lateral prone and anterior supine. A special table overlay allowed prone scintigraphy of each breast dependent through the table cut-out. All images were evaluated for abnormal Tc Sestamibi uptake prior to the patient's biopsy. Excisional biopsy of the breast lesion was obtained within six weeks of imaging. Breast pathology yielded 12 breast neoplasms and 72 benign lesions. Sestamibi breast imaging demonstrated 11 true-positives, 67 true-negatives, and 5 false positives which occurred with tracer uptake in hypercellular but benign lesions. The lone false-positive was a mammographically detected 4mm lobular carcinoma. The negative predictive value was 98.5% (67/68) and 100% in palpable lesions. This preliminary study shows that Sestamibi breast imaging can accurately exclude breast cancer in suspicious breast abnormalities.

No. 706A

ENHANCED REGIONAL CEREBRAL ACTIVATION WITH MENTAL STRESS IN CAD PATIENTS. R. Soufer, J.D. Bremner, J.A. Arrighi, M. Burg, T. Cozza, I. Cohen, H.M. Dey, D.A. Rich, B.L. Zaret, P. Goldman-Rakic, Yale University-VA Positron Imaging Laboratory, West Haven, CT.

We have previously reported that coping style is correlated with an abnormal cardiac response to a mental stress (MS) challenge in patients (pts) with CAD. This study was performed to measure functional correlates of MS in normal (n=3) and CAD (n=4) pts. Subjects underwent six 0-15 water (30 mCi) brain PET scans during 3 intervals: 2 baselines, 2 counting control (CC), 2 arithmetic (MS). PET scans were coregistered with MRI. Regions of interest were drawn on MRI scans using specific anatomical criteria. Regional activity (RA) was normalized to whole brain counts, for each scan. RA was averaged within each interval for all patients and % change in cerebral blood flow (CBF) between each interval was determined. Data for regions with the most significant change between MS and CC are shown below. There were no differences between groups in the magnitude of the increases

that occurred in heart rate and blood pressure from CC to MS.



Thus, frontal-basal ganglia-limbic circuits which have been implicated in affect, cognition and stress responsiveness are activated in CAD pts and not in normal controls during MS. These preliminary data may have important pathophysiologic implications in understanding the mechanisms and clinical expression of MS induced myocardial ischemia in CAD.

No. 660A

MYOCARDIAL PERFUSION, WALL THICKENING AND FREE FATTY ACID UPTAKE AFTER THROMBOLYSIS FOR ACUTE MYOCARDIAL INFARCTION. PR Franken, P Flamen, P Dendale, F De Geeter, H Everaert, A Momen, A Bossuyt, ML Goris *. Free University of Brussels (AZ VUB), Brussels, Belgium, and *Stanford University School of Medicine, Stanford, CA, USA.

Discrepancies between myocardial perfusion and wall thickening may be observed after acute myocardial infarction (stunned myocardium). To characterize such myocardium metabolically we compared wall motion kinetics and myocardial perfusion (using sestamibi gated SPECT) with the uptake of BMIPP, a free fatty acid analog. BMIPP uptake mainly reflects the energy dependent activation process of long chain free fatty acids prior to beta oxidation or triglyceride synthesis.

Sestamibi SPECT gated in 8 time bins and BMIPP SPECT were obtained 4-12 days after coronary thrombolysis for acute myocardial infarction in 24 patients (pts). Both tracers were injected at rest, on two separate days. Wall thickening was measured by the Stanford method. Functional, perfusion and metabolic parameters were quantified on polar maps divided into 9 regions. Results were expressed as percent of mean normal values obtained in 20 pts with low probability of CAD.

Stunned segments (segs), defined by a perfusion/ wall thickening ratio > 1.29 (normal = 1.01 ± 0.14), had a higher perfusion/ metabolic ratio (1.25 ± 0.39 vs 1.05 ± 0.14 , $p < 0.001$) indicating decreased fatty acid uptake. Fatty acid uptake was more closely related to the amplitude of wall thickening than the perfusion ($y = 34.3 + 0.80 x$; $r = 0.78$ versus $y = 62.6 + 0.55 x$; $r = 0.72$). The perfusion/ metabolic ratio was 1.05 ± 0.12 in segs with normal wall thickening, 1.21 ± 0.26 ($p < 0.001$) in segs with mild to moderate hypokinesis and 1.73 ± 0.60 ($p < 0.001$) in segs with severe dysfunction.

We conclude that soon after thrombolysis for acute myocardial infarction, wall thickening is more closely related to fatty acid uptake than to myocardial perfusion. This may indicate a relationship between decreased fatty acid metabolism and stunning.